Citation: Cell Death and Disease (2012) 3, e444; doi:10.1038/cddis.2012.184

www.nature.com/cddis

Chemotherapeutic induction of mitochondrial oxidative stress activates GSK-3α/β and Bax, leading to permeability transition pore opening and tumor cell death

F Chiara*[,1,4], A Gambalunga[1,4], M Sciacovelli[2], A Nicolli[1], L Ronconi[3], D Fregona[3], P Bernardi[2], A Rasola*[,2] and A Trevisan[1]

Survival of tumor cells is favored by mitochondrial changes that make death induction more difficult in a variety of stress conditions, such as exposure to chemotherapeutics. These changes are not fully characterized in tumor mitochondria, and include unbalance of the redox equilibrium, inhibition of permeability transition pore (PTP) opening through kinase signaling pathways and modulation of members of the Bcl-2 protein family. Here we show that a novel chemotherapeutic, the Gold(III)-dithiocarbamato complex AUL12, induces oxidative stress and tumor cell death both favoring PTP opening and activating the pro-apoptotic protein Bax of the Bcl-2 family. AUL12 inhibits the respiratory complex I and causes a rapid burst of mitochondrial superoxide levels, leading to activation of the mitochondrial fraction of GSK-3α/β and to the ensuing phosphorylation of the mitochondrial chaperone cyclophilin D, which in turn facilitates PTP opening. In addition, following AUL12 treatment, Bax interacts with active GSK-3α/β and translocates onto mitochondria, where it contributes to PTP induction and tumor cell death. These findings provide evidence that targeting the redox equilibrium maintained by mitochondria in tumor cells allows to hit crucial mechanisms that shield neoplasms from the toxicity of many anti-tumor strategies, and identify AUL12 as a promising chemotherapeutic compound.

Cell Death and Disease (2012) **3,** e444; doi:10.1038/cddis.2012.184; published online 13 December 2012
Subject Category: Internal medicine

Neoplasms acquire the capability to grow in a rapid and deregulated way under the strong selective pressure of stressful conditions, as they adopt flexible molecular strategies to overcome the multiplicity of apoptotic signals and environmental constraints they encounter.[1,2] This high degree of biological plasticity makes cancer cells an elusive target for most therapies, and urges to define specific biological traits of malignant cells that could be utilized for tailored pharmacological approaches.

Several biochemical changes that crucially contribute to neoplastic transformation take place in mitochondria. In most cases, it is in mitochondria that cell commitment to death reaches the point of no return. Opening of the mitochondrial permeability transition pore (PTP), a large channel located in the inner mitochondrial membrane, results in mitochondrial depolarization, swelling, Ca^{2+} release, rupture of the outer membrane and delivery of proteins that trigger the executioner phase of apoptosis.[3] Release of these effector proteins from mitochondria can also occur following the insertion/oligomerization in the outer mitochondrial membrane of pro-apoptotic members of the Bcl-2 family protein, such as Bax or Bak.[4] Mitochondria of tumor cells undergo changes that contribute to the build-up of solid anti-apoptotic defences. Expression levels of Bcl-2 family proteins are altered, or they are targeted by a myriad of post-translational modifications driven by oncogenic signaling pathways,[4,5] with an increase of anti-apoptotic or a decrease of pro-apoptotic functions. A reduced sensitivity of mitochondrial PTP to diverse stress stimuli was also observed in neoplastic cells,[3,6] and we and others have recently found that PTP opening is enhanced by a GSK-3α/β-dependent phosphorylation of the chaperone cyclophilin D (CyP-D), a well-known regulator of the PTP, and that this pathway is inhibited in cancer cells.[7–9]

During the progression to malignancy, neoplastic accrual overgrows the supply of oxygen and nutrients provided by surrounding blood vessels.[10] To avoid the noxious effect of

[1]Department of Molecular Medicine, University of Padova, Padova, Italy; [2]CNR Institute of Neuroscience and Department of Biomedical Sciences, University of Padova, Padova, Italy and [3]Department of Chemical Sciences, University of Padova, Padova, Italy
*Corresponding author: Dr F Chiara, Department of Molecular Medicine, University of Padova, Via Giustiniani 2, I-35128 Padova, Italy. Tel: +39 049 821 1371; Fax: +39 049 821 2542. E-mail: federica.chiara@unipd.it
or A Rasola, CNR Institute of Neuroscience and Department of Biomedical Sciences, Viale G. Colombo 3, I-35121, Padova, Italy, Tel: +39 049 827 6062; Fax: +39 049 827 6361. E-mail: andrea.rasola@unipd.it
[4]These two authors equally contributed to this work.
Keywords: chemotherapeutics; permeability transition pore; oxidative stress; apoptosis; cancer
Abbreviation: AUL12, ([AuIIIBr2(ESDT)]; ESDT, ethylsarcosinedithiocarbamate); BIP, Bax inhibiting peptide; CRC, Ca^{2+} retention capacity; CsA, cyclosporin A; CyP-D, cyclophilin D; HK II, hexokinase isoform II; IND, indirubin-3'-oxime; NAC, *N*-acetyl-L-Cysteine; OCR, oxygen consumption rate; OXPHOS, oxidative phosphorylation; PTP, permeability transition pore; RC, respiratory chain; ROS, reactive oxygen species
Received 26.9.12; revised 29.10.12; accepted 05.11.12; Edited by G Raschellà

these hypoxic conditions, cells in the tumor mass interior enhance glucose utilization (the Warburg effect;[11–13]), with a concomitant decrease of mitochondrial respiration.[14] This inhibition of respiratory chain (RC) complexes can increase reactive oxygen species (ROS) production,[15] and above a certain threshold, oxidative stress can damage a variety of cellular structures and eventually prompt cell death by triggering PTP opening through poorly defined mechanisms.[16] Cancer cells are therefore forced to concomitantly induce anti-oxidant defences to set a novel homeostatic redox equilibrium,[17–19] and further increases in ROS levels could overwhelm their residual anti-oxidant capabilities. In contrast, the same degree of oxidative stress could be more easily managed by non-transformed cells. Thus, targeting the redox equilibrium constitutes a promising strategy in the development of new and selective anticancer strategies, on the basis of drugs that eliminate neoplastic cells by increasing mitochondrial ROS to levels able to unlock PTP desensitization.

In this conceptual framework, we have investigated the molecular mechanisms of action of a derivative of Gold(III)-dithiocarbamato family compounds, named AUL12 ((AuIII-Br2(ESDT)), ESDT: ethylsarcosinedithiocarbamate), whose design is aimed at identifying metal-dithiocarbamato derivatives that resemble cisplatin, but are endowed with a higher anticancer activity, improved selectivity and bioavailability and lower side effects.[20] Gold(III)-dithiocarbamato agents have outstanding cytotoxicity levels *in vitro* toward a number of human tumor cell lines.[21] AUL12 was selected among this class of molecules for its efficacious anti-neoplastic activity, both *in vitro*, as it kills cancer cells by increasing intracellular ROS levels,[22] and *in vivo* toward several cancer xenografts, including some obtained with cisplatin-resistant prostate cancer cells,[23,24] and for its extremely low nephrotoxicity and acute toxicity.[24]

Here we have characterized the mechanism of action of AUL12, finding that it inhibits RC complex I, raising ROS levels and activating GSK-3α/β. Active GSK-3α/β prompts tumor cell death, both facilitating PTP opening and causing Bax redistribution to mitochondria. Our data indicate that a survival platform that functionally connects RC complexes, the redox balance, kinase signaling and mitochondrial death executioners can be targeted in neoplastic cells in order to obtain their selective clearing.

Results

AUL12 induces dose-dependent cell death. In order to understand the mechanism of cytotoxicity of AUL12, we first characterized its effects on viability in: (a) a model of highly aggressive cancer cells, the human osteosarcoma SAOS-2 cells, characterized by loss of p53 activity; (b) the human epithelial prostate cells RWPE-1, which are immortalized but lack any tumorigenic potential, and (c) the RWPE-2 cells, which are made tumorigenic by expression of K-Ras in RWPE-1 cells.[25,26] AUL12 treatment resulted in a rapid (3 h) dose- and time-dependent raise of mitochondrial superoxide levels in SAOS-2 cells (Supplementary Figure. 1a), which was paralleled by a massive mitochondrial depolarization and cell death induction in the same ambit of drug dose and time (Figure 1a, b). In RWPE cells, K-Ras transformation significantly enhanced cell death induced by AUL12 (compare Supplementary Figure 2a and 2b). Pre-treating cells with the anti-oxidant *N*-acetyl-L-Cysteine (NAC) prevented mitochondrial depolarization (Figure 1a) and cell death (Figure 1b and Supplementary Figure 2a and 2b), demonstrating the ROS-dependency of AUL12 toxicity. By contrast, the reference drug cisplatin failed to induce cell death after a 3-h incubation (Supplementary Figure 3a), whereas it triggered a NAC-insensitive cell death after 24 h (Supplementary Figure 3b). Taken together, these results indicate that the two metal-based compounds damage cells through different mechanisms, and that AUL12 prompts a rapid cell death by increasing mitochondrial ROS levels.

AUL12 inhibits RC complex I and elicits ROS production. Mitochondrial RC complexes I, II and III are among the main sources of intracellular ROS,[15] and their targeting by AUL12 could inhibit oxygen consumption rate (OCR) and boost ROS levels in tumor cells. We observed that a 15-min pre-treatment with AUL12 inhibited in a dose-dependent fashion both coupled respiration and total mitochondrial OCR, up to a complete abrogation of any mitochondrial oxygen consumption (Figure 2a, right and left panel).

To dissect the effect of AUL12 on respiration, we directly tested maximal RC complex activity under conditions where complexes are made accessible in mitochondria or permeabilized cells, and exposed to an excess of substrates. AUL12 exerted a modest inhibitory effect on RC complex II/III (Figure 2b), whereas it completely abolished RC complex I activity both in mitochondria and permeabilized cells (Figures 2c and d). The lack of an additive effect on the rise of mitochondrial ROS levels between the complex I inhibitor rotenone and AUL12 (Supplementary Figure 1b) further indicates that AUL12 increases ROS by targeting complex I.

AUL12 sensitizes the permeability transition pore to opening. It is postulated that ROS increase intracellular Ca^{2+}, which in turn would augment ROS generation, in a feed-forward circuit eventually leading to PTP opening and cell death.[16,27,28] In cancer cell models, PTP opening is made more difficult by a constitutive GSK-α/β inhibition, which acts as a solid survival mechanism.[8]

In order to investigate whether AUL12 influences the pore, we used a whole-cell Ca^{2+} retention capacity (CRC) assay, which evaluates the modulation of PTP opening through the assessment of the amount of Ca^{2+} taken up by mitochondria of digitonin-permeabilized cells.[29] A 3-h treatment with AUL12 elicited a dose-dependent CRC shortening, that is, an induction of PTP opening, both on cells (Figures 3a and b) and on isolated liver mitochondria (Figures 3c and d). This induction was totally prevented by the anti-oxidant NAC (Figures 3e and f), whereas the addition to permeabilized cells of cyclosporin A (CsA), an inhibitor of the pore regulator CyP-D, markedly increased the amount of Ca^{2+} required to open the PTP (Figures 3a and b).

GSK-3α/β activation mediates the biological effects of AUL12. These data indicate that AUL12 can rapidly induce inhibition of RC Complex I and oxidative stress, unlocking the

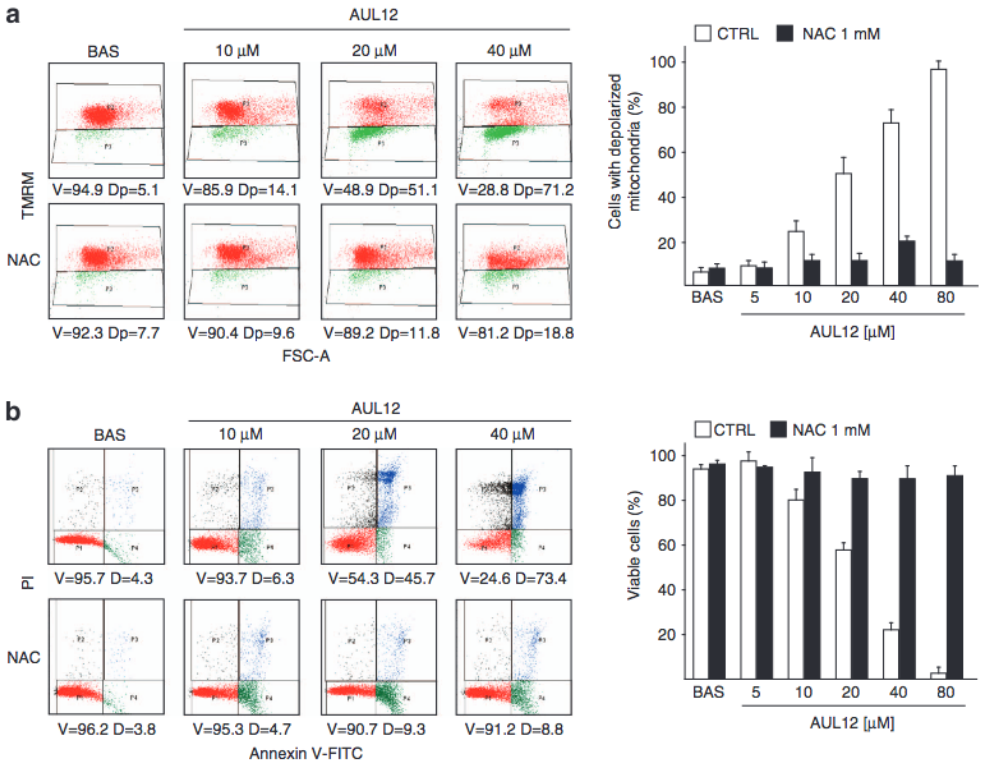

Figure 1 AUL12 induces mitochondrial depolarization and cell death through mitochondrial superoxide production. (**a**) Cytofluorimetric analysis (Forward Scatter, FSC, *versus* Tetramethylrhodamine methyl ester, TMRM) showing mitochondria depolarization in human osteosarcoma SAOS-2 cells exposed to AUL12. One representative experiment is reported on the left, in which viable cells (V, TMRM positive) are delimited by the upper quadrant, and cells displaying depolarized mitochondria (Dp) are delimited by the lower quadrant. (**b**) Death induction on SAOS-2 cells exposed to AUL12 is shown as cytofluorimetric analysis of propidium iodide (PI) *versus* Annexin V-FITC staining. On the left, one representative experiment is reported. Viable cells (V, double negative for PI and Annexin V-FITC) are delimited by the lower left quadrants; early apoptotic cells (Annexin V-FITC single positive) are in the lower right quadrants; late apoptotic and/or necrotic cells (PI and Annexin V-FITC double positive) are in the upper right quadrants; necrotic cells (PI single positive) are in the upper right quadrants. D (dead) indicates the sum of all apoptotic and necrotic cells. Both in (**a**) and in (**b**), data quantification is in the bar graphs on the right; values are the mean ± S.D. of at least five experiments. All along the figure, numbers in plots are percentages; AUL12 was incubated for 3 h; *N*-acetyl cysteine (NAC, 1 mM) was pre-incubated 1 h before AUL12 treatment

mitochondrial PTP of tumor cells in a ROS-dependent way. In tumor cells, a condition that markedly induce the PTP is GSK-3α/β activation.[6] We found that increasing doses of AUL12 elicit a marked and NAC-sensitive raise of GSK-3α/β activity[30] (Figure 4a). Furthermore, cell pre-incubation with the GSK-3α/β inhibitor indirubin-3′-oxime before AUL12 treatment both abrogated PTP sensitization (Figure 4b) and protected cells from apoptosis (Figure 4c). Therefore, AUL12 activates GSK-3α/β in a ROS-dependent fashion, and GSK-3α/β activation in turn induces PTP opening. GSK-3α/β inhibition by activation of survival kinase signaling favors the recruitment of the isoform II of hexokinase (HK II) onto the mitochondrial surface of tumor cells,[31,32] where it diminishes PTP sensitivity to stress stimuli.[29] However, we found that the level of HK II bound to mitochondria was not changed by AUL12 treatment (data not shown). Another possible mechanism of pore regulation by GSK-3α/β was phosphorylation of the PTP regulator CyP-D by the mitochondrial fraction of the kinase, thus enhancing PTP opening. Accordingly, we found that AUL12 activates mitochondrial GSK-3α/β (Figure 4d) and induces CyP-D phosphorylation (Figure 4e).

GSK-3α/β also triggers cell death through mitochondrial circuits alternative to PTP opening, such as mitochondrial translocation of the pro-apoptotic Bcl-2 family member Bax,[33] which leads to permeabilization of the outer mitochondrial membrane. Co-immunoprecipitation experiments revealed that Bax and active, Tyr-phosphorylated GSK-3α/β interacts in cells treated with AUL12, and this interaction was abrogated by cell pre-treatment with either indirubin-3'-oxime or the antioxidant NAC (Figure 5a and b). Moreover, we observed that AUL12 induces Bax translocation to mitochondria, and this process is inhibited by the GSK-3α/β inhibitor indirubin-3′-oxime (Figure 5c). Notably, cell pre-treatment with a selective Bax-inhibiting peptide (BIP) could partially inhibit pore opening induced by AUL12 (Figure 5d) and protected tumor cells from AUL12 lethality (Figure 5e). Taken together, these findings indicate that the increased intracellular ROS levels elicited by AUL12 activate GSK-3α/β, which in turn triggers cell death through mitochondrial membrane permeabilization mediated both by PTP opening and by Bax recruitment on mitochondria, which could contribute to pore induction.

Discussion

In the present work, we have characterized the biochemical mechanisms sustaining the anticancer action of AUL12, a new chemotherapeutic of the Gold(III)-dithiocarbamato family.

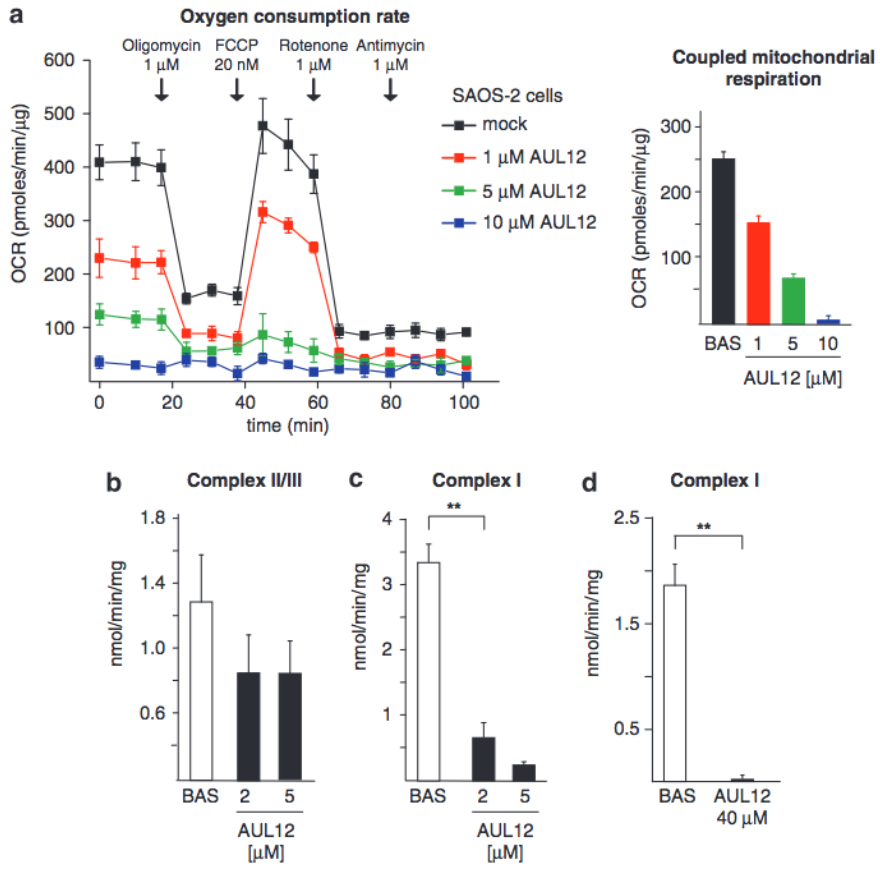

Figure 2 AUL12 inhibits OCR and RC complex I. (**a**) On the right, representative traces of OCR measurements performed on monolayers of living SAOS-2 cells treated with AUL12. Subsequent additions of the ATP synthase inhibitor oligomycin, of the uncoupler FCCP, of the RC complex I inhibitor rotenone and of the RC complex III inhibitor antimycin A were carried out. AUL12 at the reported concentrations was pre-incubated 15 min before starting the experiments. Bar graphs on the right show the coupled mitochondria respiration, which was calculated by subtracting the uncoupled mitochondrial OCR from the basal OCR (after and before oligomycin addition, respectively) after having detracted the non-mitochondrial component of OCR (the rotenone/antimycin insensitive OCR fraction). The enzymatic activity of RC complexes II–III (**b**) or of RC complex I (**c**) was evaluated on mitochondria isolated from SAOS-2 cells in the presence or absence of different concentrations of AUL12 added 5 min before starting the experiment. In (**d**), the activity of RC complex I was analyzed on permeabilized SAOS-2 cells pre-treated or not for 90 min with 40 μM AUL12. All data of RC complex activity were normalized to the citrate synthase activity and are mean ± S.D. values ($n = 6$). Statistical significance was measured with a Student's *t* test and is indicated by asterisks (**$P < 0.005$)

We have found that AUL12 strongly inhibits the activity of the RC Complex I and causes a rapid raise in ROS levels, which in turn lead to mitochondrial PTP opening and cancer cell apoptosis. The role played by oxidants in neoplastic transformation is complex and not fully understood. ROS may contribute in stimulating proliferation, invasion and metastasis and in inhibiting apoptosis.[34] By inducing genomic instability, ROS accelerate the rate of mutations and lead to further neoplastic alterations, such as dysfunctions in energy metabolism, with leakage of electrons during the oxidative phosphorylation process and the ensuing generation of superoxide and subsequently hydrogen peroxide.[18,35,36] Activation of several oncogenes, such as Ras, Bcr-Abl and c-Myc or loss of functional p53 increase ROS production by enhancing glycolysis and inhibiting oxidative phosphorylation.[37–39] These alterations are postulated to make tumor cells vulnerable to a further oxidative stress. Accordingly, we have found that human osteosarcoma SAOS-2 cells, which lack a functional p53,[40] undergo a massive apoptosis after 3 h of AUL12 treatment.

However, the interplay between pro-neoplastic signal transduction and redox regulation can be complex, as in the case of the K-Ras oncogene: a low level of K-Ras expression promotes a ROS detoxification program required for tumor initiation, proliferation and survival,[19] but a marked increase in its activity boosts mitochondrial ROS, which stimulate cellular proliferation and anchorage-independent growth,[41] and drugs such as lanperisone or erastin induce mitochondrial release of ROS, oxidative cell death and tumor growth suppression in oncogenic model harboring oncogenic K-Ras mutations.[42,43] Consistent with a K-Ras sensitization to oxidative stress, AUL12 is more effective in inducing apoptosis in the K-Ras-transformed RWPE-2 prostate epithelial cells than in the non-transformed parental RWPE-1 cells, although these are more sensitive to a variety of apoptogenic stimuli.[8] In addition, AUL12 inhibits the xenographic growth of prostate tumor cells *in vivo*, causing minimal systemic toxicity.[23]

However, above a certain threshold, oxidative stress may induce a prolonged opening of the mitochondrial PTP, irreversibly committing cells to death. A rise in ROS levels

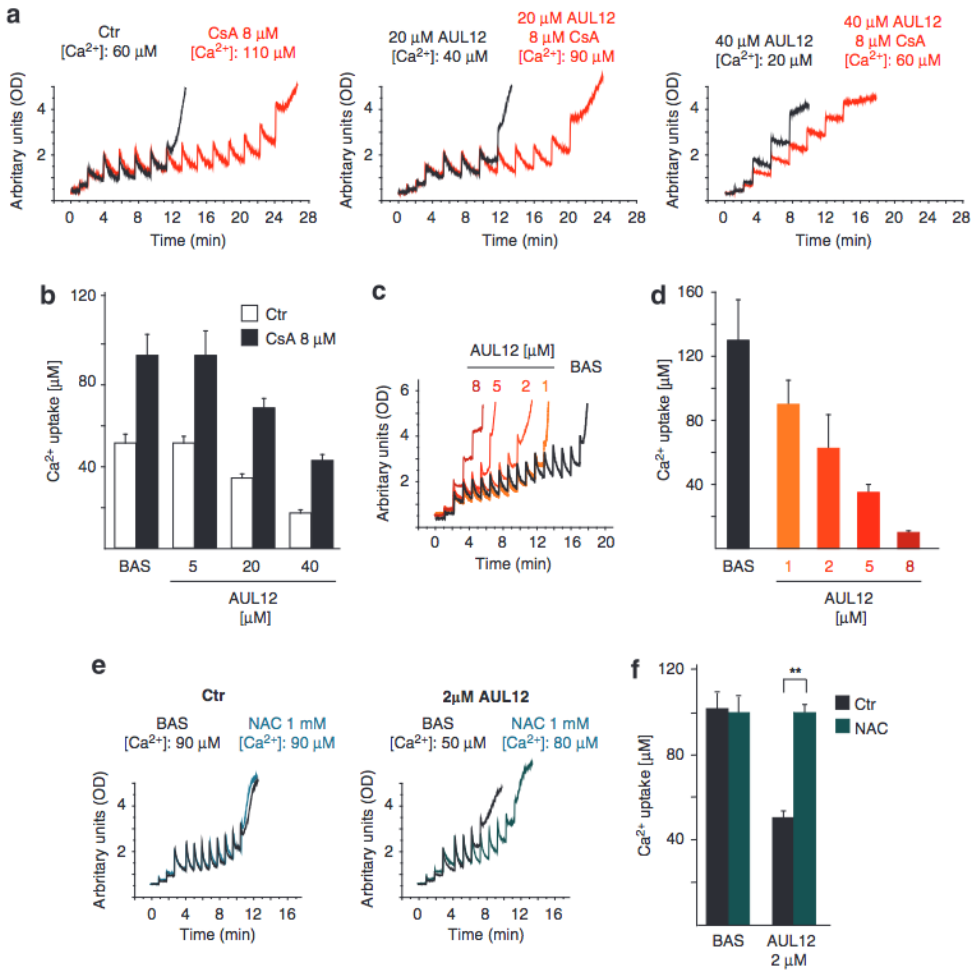

Figure 3 AUL12 sensitizes the PTP to opening in a ROS-dependent way. (**a**) PTP opening of SAOS-2 cells treated with AUL12 is measured with the whole-cell CRC assay. Fluorescence of Calcium Green-5N in digitonin-permeabilized cells is reported as arbitrary units on the *y* axis. As the probe does not permeate mitochondria, Ca^{2+} uptake into the organelles after each pulse (5 µM Ca^{2+}) is displayed by a rapid decrease of the fluorescence spike. Pore inhibitors and inducers are expected to increase or decrease, respectively, the number of spikes before permeability transition, that is, a sudden and marked fluorescence increase, occurs. AUL12 was added to cells at the indicated concentrations 3 h before permeabilization with digitonin. Where indicated, cyclosporine A (CsA) was added 5 min before starting the assay. The bar graphs in (**b**) report the total Ca^{2+} uptake before PTP opening (results are mean ± S.D.; $n=6$). (**c, e**) Representative CRC experiments performed on isolated liver mitochondria treated with different concentrations of AUL12 (**c**) and/or with *N*-acetyl-cysteine (NAC, 1 mM; (**e**)). The bar graphs in (**d, f**) report the total Ca^{2+} uptake before PTP opening (results are mean ± S.D.; $n=6$). Statistical significance was measured with a Student's *t* test and is indicated by asterisks (**$P<0.005$)

can trigger a feed-forward loop involving a progressive Ca^{2+} surge, a further ROS increase and prolonged PTP openings,[16,27,28] but the molecular mechanisms promoting this process and their possible deregulation in cancer remain poorly defined. Most of the ROS generated in intact mitochondria are contributed by RC Complex I,[44] a NADH: Quinone Oxidoreductase endowed with an extremely complex structure.[45] A fine regulation of Complex I activity occurs during tumorigenesis. For instance, K-Ras-transformed fibroblasts decrease Complex I content and activity, as compared with a control counterpart.[46] The quinone analog rotenone increases superoxide production from NAD^+-linked substrates, and interferes with the formation of a stabilized ubisemiquinone in the matrix part of the complex.[34] As we observe that ROS induced by AUL12 are not further increased by rotenone, we suspect that the two drugs act on the same biochemical process within Complex I. Notably, rotenone-dependent oxidative stress elicits autophagic death in cancer cells.[47]

ROS recruit and tune the activity of signaling molecules in a highly compartmentalized fashion within the cell.[48] ROS-sensitive proteins regulate a variety of cellular functions that are relevant in tumor onset and development.[35] We observe that the oxidative stress elicited by AUL12 causes phosphorylation of the Tyr(279/216) residue on GSK-3α/β, which activates the enzyme and favors its subcellular redistribution.[49] A ROS-dependent activation of GSK-3α/β was observed in several cell models, including cardiomyocytes through sustained ERK[50] or mTOR[51] activation, mesangial cells, where a ROS-GSK-3α/β signaling pathway induces autophagy,[52] or neuronal cells, in which oxidative stress elicits a marked activation of GSK-3β that antagonizes survival signals.[53] GSK-3α/β can favor PTP opening either by promoting HK II detachment from mitochondria,[29,31,32] or by

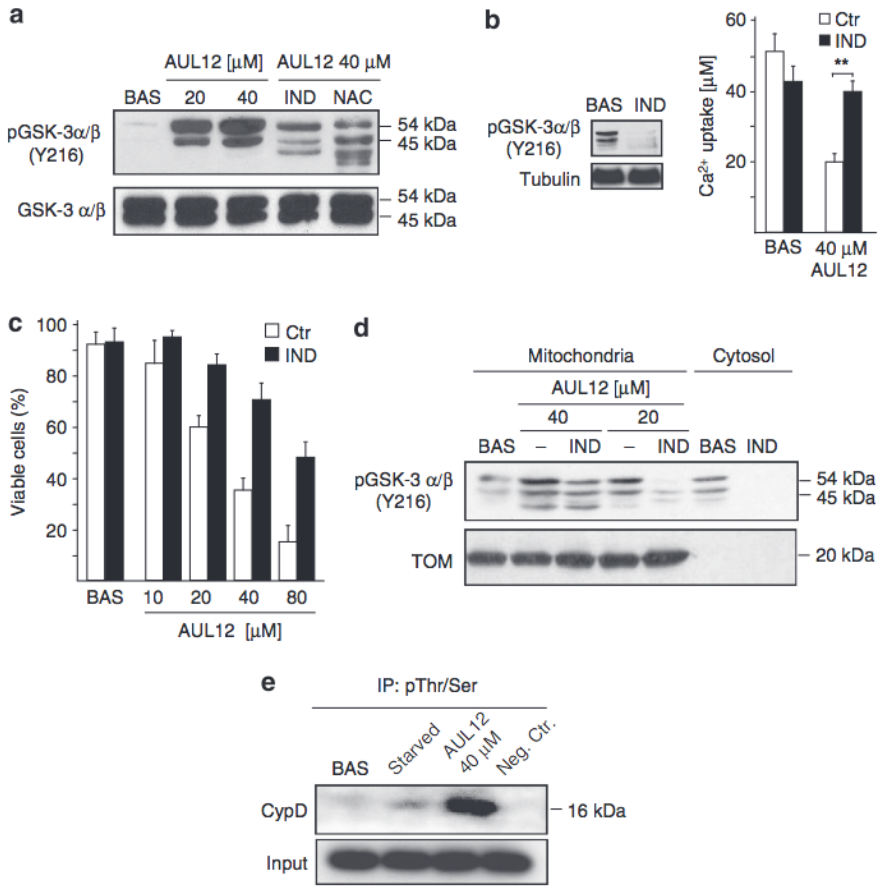

Figure 4 AUL12 induces cells death through ROS-dependent activation of GSK-3α/β. (**a**) Western immunoblotting analysis showing phosphorylation of the activator Y(279/216) residue of GSK-3α/β in total SAOS-2 cell lysates. Where indicated, cells were treated with AUL12 (2 h) and pre-incubated with NAC (1 mM, 1 h) or with the GSK-3α/β inhibitor indirubin (IND, 2 μM, 3 h) before exposure to AUL12. (**b**) CRC experiments on whole cells treated or not with AUL12 (40 μM, 2 h) show that pre-treatment with indirubin (IND) rescues PTP opening induced by the chemotherapeutic. Mitochondrial Ca^{2+} uptake in the various conditions is compared with that measured in unstimulated cells. In the inset, the efficacy of indirubin to inactivate GSK-3α/β is shown as dephosphorylation of the Y(279/216) residue. (**c**) Death induction on SAOS-2 cells exposed to different concentrations of AUL12 with or without pre-incubation with IND is analyzed by cytofluorimetry with a propidium iodide/Annexin V-FITC double staining, as in Figure 1B. Viable cells reported in the bar graph are negative for both fluorophores. (**d**) Western immunoblotting analysis of phospho-Y(279/216) GSK-3α/β residue in mitochondrial and cytoplasmic fractions of SAOS-2 cells exposed to AUL12 with or without pre-incubation with IND. (**e**) Immunoprecipitation of anti-phospho-serine/threonine residues from mitochondria of SAOS-2 cells exposed to serum starvation (24 h) or to AUL12 was followed by Western immunoblotting analysis of cyclophilin D. All along the figure, bar graphs report mean ± S.D. values ($n = 3$). Statistical significance was measured with a Student's *t* test and is indicated by asterisks (**$P < 0.005$). The inhibitor IND (2 μM) was preincubated for 3 h

phosphorylating the chaperone and PTP regulator CyP-D,[7–9] and in neoplasms, several oncogenic signals converge on mitochondrial GSK-3α/β to maintain the PTP locked.[6] Here we determine that ROS-dependent GSK-3α/β activation does not change the HK II-binding equilibrium with mitochondria, but it phosphorylates CyP-D, functionally connecting AUL12-dependent GSK-3α/β activation with PTP induction.

In parallel, we have observed that ROS raised by AUL12 induce an interaction between GSK-3α/β and the pro-apoptotic Bcl-2 family protein Bax, with a dramatic relocation of Bax on mitochondria. This result is in accordance with previous observations, showing that GSK-3α/β can activate Bax either directly, by phosphorylation on Ser-163 or by promoting its p53-induced expression.[33] Mitochondrial Bax induces cell death, prompting permeabilization of the outer membrane and the subsequent release of apoptogenic factors.[54] However, functional connections between Bax and PTP regulation have also been proposed, as it was shown that Bax blocks a voltage-dependent K^+ channel termed $K_V1.3$ in the inner mitochondrial membrane, leading to rapid ROS production and PTP opening.[55] Accordingly, we observe that Bax inhibition with a selective peptide partially rescues PTP opening and cell death elicited by AUL12.

The mechanisms by which AUL12 targets the unbalanced homeostatic redox equilibrium of malignant cells allow to shed light into the mitochondrial machinery that orchestrates neoplasm survival. The functional connection we observe among Complex I, enhanced ROS production, activation of GSK-3α/β and Bax and unlocking of the PTP offers multiple, promising therapeutic targets. Treatment-derived toxicity, cell-insensitivity to drugs and lack of therapeutic selectivity are still major issues in developing strategies leading to cancer cure. Given its ability to selectively kill cancer cells *in vivo* and *in vitro* without systemic toxicity, AUL12 could

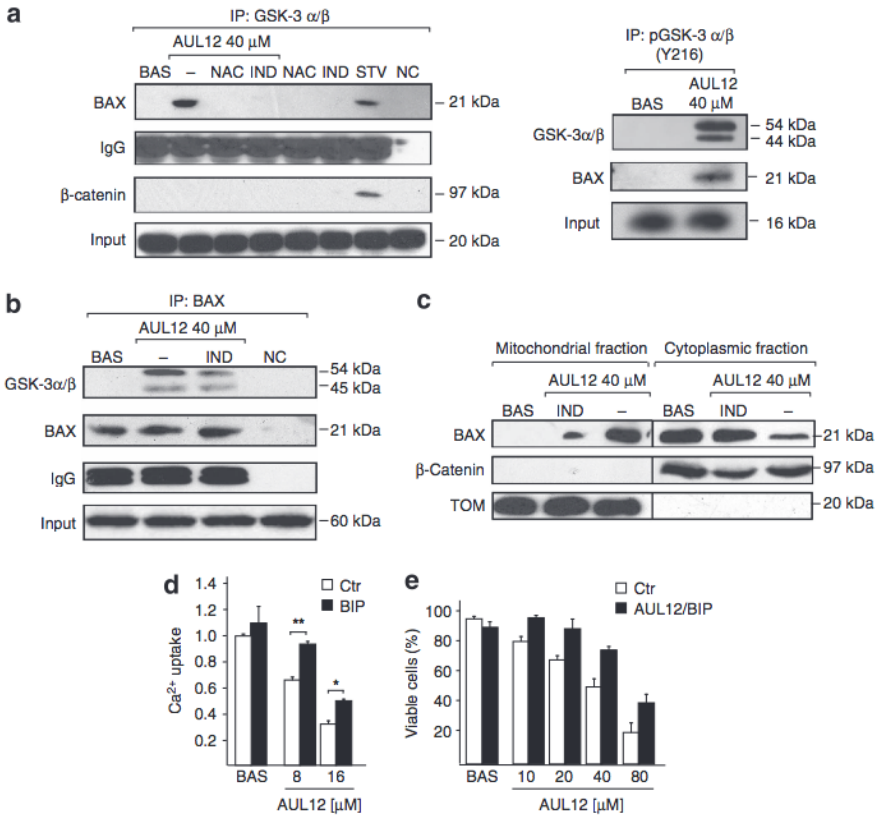

Figure 5 AUL12 induces an interaction between phosphorylated GSK-3α/β and Bax, which translocates onto mitochondria and contributes to PTP induction and cell death. (**a**) On the left, GSK-3α/β immunoprecipitation in SAOS cells treated or not for 2 h with 40 μM AUL12; where indicated, cells were pre-incubated with IND (2 μM, 3 h) or NAC (1 mM, 1 h). The Western immunoblot was probed with Bax, whereas β-catenin is used as a positive control of co-immunoprecipitation with GSK-3α/β in starved cells (STV); NC, negative control. On the right, p(Y216)GSK-3α/β immunoprecipitation in SAOS cells treated or not for 2 h with 40 μM AUL12. The Western immunoblot was probed with GSK-3α/β and Bax. In both panels, IgG is used as a loading control. (**b**) Bax immunoprecipitation in SAOS cells treated or not for 2 h with 40 μM AUL12; where indicated, cells were pre-incubated with IND, as in (**a**). The Western immunoblot was probed with GSK-3α/β with Bax, and with IgG as a loading control; NC, negative control. (**c**) Western immunoblot on cytosolic and mitochondrial fractions of SAOS-2 cells treated or not for 2 h with 40 μM AUL12; where indicated, cells were pre-incubated with IND, as in (**a**). To check for fraction purity, the blot was also probed with β-catenin as a cytosolic marker and with TOM20 as a mitochondrial marker. (**d**) CRC experiments on whole cells treated with the reported concentrations of AUL12 (with or without a 1 h of preincubation with a Bax inhibiting peptide (BIP, 60 μM). Mitochondrial Ca^{2+} uptake in the various conditions is compared with that measured in unstimulated cells. (**e**) Death induction on SAOS-2 cells exposed to different concentrations of AUL12 with or without pre-incubation with the BIP (60 μM) is analyzed by cytofluorimetry with a propidium iodide/Annexin V-FITC double staining, as in Figure 1b. Viable cells reported in the bar graph are negative for both fluorophores. All along the figure, bar graphs report mean ± S.D. values ($n=3$). Statistical significance was measured with a Student's *t* test and is indicated by asterisks (*$P<0.01$, **$P<0.005$)

constitute a leading compound in the development of chemotherapeutics that target the unique neoplastic alterations of the cell redox equilibrium.

Materials and Methods

Chemicals and reagents. FITC-conjugated Annexin-V was from Roche (Indianapolis, IN, USA); Calcium Green-5N and tetramethylrhodamine methyl ester (TMRM) were from Molecular Probes (Eugene, OR, USA); PD 98059 and Indirubin-3-monoxime were from Calbiochem (San Diego, CA, USA); all other chemicals (oligomycin, antimycin, rotenone, *N*-acetyl-L-Cysteine (NAC)) were from Sigma (St. Louis, MO, USA). The mouse monoclonal anti-actin antibody (input) was from Sigma; the mouse monoclonal anti-GSK-3α/β, the rabbit polyclonal anti-BAX and anti-TOM20 antibodies were from Santa Cruz Biotechnology (Santa Cruz, CA, USA), the monoclonal anti-CyP-D antibody was from Calbiochem; rabbit anti-phospho-Y(279/216) GSK-3α/β antibodies were from Cell Signalling (Beverly, MA, USA); FITC-conjugated secondary antibodies were from Sigma. *N*-acetyl-L-Cysteine (NAC), was added 1 h before starting apoptosis induction by AUL12, whereas IND was added 3 h before.

Flow cytometry analysis of apoptosis induction. Flow cytometry recordings of apoptotic changes were performed, as described.[56,57] Briefly, after induction of apoptosis, cells were resuspended in 135 mM NaCl, 10 mM HEPES, 5 mM $CaCl_2$ and incubated for 15 min at 37 °C in FITC-conjugated Annexin-V, TMRM (20 nM) and propidium iodide (PI, 1 $\mu g\,ml^{-1}$), to detect mitochondrial depolarization (reduced TMRM staining), phosphatidylserine exposure on the cell surface (increased FITC-conjugated Annexin-V staining) and loss of plasma membrane integrity (PI permeability and staining). Samples were analyzed on a FACS Canto II flow cytometer (Becton Dickinson, San Diego, CA, USA). Data acquisition and analysis were performed using FACSDiva software (Becton Dickinson). Each experiment was repeated at least four times, and consistency of data allowed to show one representative experiment for each condition.

Cell lysis, fractionation and western immunoblot analysis. Total cell extracts were prepared at 4 °C in 140 mM NaCl, 20 mM Tris-HCl (pH 7.4), 5 mM EDTA, 10% glycerol and 1% Triton X-100 in the presence of phosphatase and protease inhibitors (Sigma). To separate mitochondria from the cytosolic fraction, cells were placed in an isolation buffer (250 mM sucrose, 10 mM Tris-HCl, 0.1 mM EGTA-Tris, pH 7.4) and homogenized at 4 °C. Mitochondria were then isolated by differential centrifugation (three times, first at 700 × *g* and twice at 9000 × *g*, all at 4 °C, 10 min) in mitochondrial isolation buffer.

For immunoprecipitations, 2000–3000 μg of proteins per reaction were incubated with antibodies conjugated to protein A- or protein G-Sepharose beads (Sigma) at 4 °C overnight. Negative controls were performed by incubating lysates on

conjugated beads in the absence of primary antibodies. Samples were then separated in reducing conditions on SDS-polyacrylamide gels and transferred onto Hybond-C Extra membranes (Amersham, Little Chalfont, UK). Primary antibodies were incubated for 16 h at 4 °C, and horseradish peroxidise-conjugated secondary antibodies were added for 1 h. Western immunoblots were carried out under standard conditions, and proteins were visualized by enhanced chemiluminescence (Millipore, Billerica, MA, USA).

Isolation of mouse mitochondria. Mitochondria were isolated from livers of wild-type, BALBc mice, through sequential centrifugations, as described.[58] All procedures were carried out at 4 °C.

Measurement of mitochondrial Ca^{2+} retention capacity. The CRC assay was used to assess PTP opening following trains of Ca^{2+} pulses[29,58] and measured fluorimetrically at 25 °C in the presence of the Ca^{2+} indicator Calcium Green-5N (1 μM; λ exc: 505 nM; λ nM: 535 nM; Molecular Probes). We performed CRC experiments either on isolated mitochondria or on whole cells placed in an isotonic buffer (130 mM KCl, 1 mM Pi-Tris (Pi: inorganic phosphate), 10 mM Tris/MOPS, 10 μM EGTA/Tris, 5 mM glutamate/2,5 mM malate, 10 μM cytochrome *c*, pH 7.4). Whole cells CRC was carried out after plasma membrane permeabilization with the non–ionic detergent digitonin, which is highly selective for cholesterol-enriched membranes and does not damage the mitochondrial membranes. Cells were washed twice in a buffer composed of 130 mM KCl, 1 mM Pi-Tris, 10 mM Tris/MOPS, 1 mM EGTA/Tris, pH 7.4 and then permeabilized with 150 μM digitonin (15 min, 4 °C) in the same buffer with modified EGTA/Tris, (1 mM, pH 7.4). Digitonin was then washed away by spinning cells twice in the washing buffer with 0.1 mM EGTA/Tris, and the number of cells carefully assessed before starting each experiment. Mitochondria (0,5 mg ml^{-1}) or permeabilized cells (7×10^6 cells per experiment) were then placed in the presence of the Ca^{2+} indicator Calcium-Green-5N, which does not permeate mitochondria, and exposed to Ca^{2+} spikes (10 μM and 5 μM, respectively). Fluorescence drops were used to assess mitochondrial Ca^{2+} uptake. PTP opening was detected as a fluorescence increase.

Determination of mitochondrial respiratory complex activity. To measure the enzymatic activity of RC complexes, mouse liver mitochondria were homogenized with an electric potter (Sigma) in a buffer composed by 250 mM sucrose, 10 mM Tris-HCl, 0.1 mM EGTA-Tris, pH 7.4, Percoll 10%, protease and phosphatase inhibitors and mitochondria isolated, as described above with different centrifugations. The activities of mitochondrial respiratory complex I and II/III were determined spectrophotometrically, as described.[59] Briefly, for complex I mouse liver mitochondria (40 μg ml^{-1}) were placed in an assay medium composed by Tris 10 mM pH 8, bovine serum albumin 3 mg ml^{-1}, alamethicin 5 μM, sodium azide 5 mM, antimycin 1 μM, CoQ 6,5 μM and the absorbance change (340 nM, 37 °C) with or without AUL12(10 min. incubation) was recorded for 1 min. Then NADH (0,1 mM) was added, and the NADH oxidoreductase activity was measured for 5 min before the addition of rotenone (20 μM) after which the activity was measured for an additional 3 min. Complex I activity is the rotenone-sensitive NADH oxidoreductase activity.

For the determination of complex II/III activities, mouse liver mitochondria (40 μg ml^{-1}) were placed in a medium composed of KH_2PO_4 25mM, bovine serum albumin 1 mg ml^{-1}, sodium azide 5 mM, succinate 10 mM, alamethicin 5 μM, ATP 0,1 mM with or without AUL12 (10-min incubation). Then cytochrome *c* 50 μM was added and the decrease of absorbance (550 nM, 37 °C) recorded for 10 min. Finally, the data were corrected for the activity of citrate synthase:mouse liver mitochondria (40 μg ml^{-1}) were placed in a medium composed by Tris/HCl 100mM, pH = 8, DTNB 0,1 mM, acetyl CoA 0,3mM and oxaloacetate 0,5 mM. The increase of absorbance (412 nM, 37 °C) was then recorded for 10 min.

Oxygen consumption rate (OCR) experiments. The rate of oxygen consumption was assessed in real-time with the XF24 Extracellular Flux Analyzer (Seahorse Biosciences), which allows to measure OCR changes after up to four sequential additions of compounds. Cells (5×10^4 per well) were plated the day before the experiment in a DMEM/10% serum medium; experiments were carried out on confluent monolayers. Before starting measurements, cells were placed in a running DMEM medium (supplemented with 25 mM glucose, 2 mM glutamine, 1 mM sodium Pyruvate, and without serum) and pre-incubated for 1 h at 37 °C in atmospheric CO_2. OCR values were then normalized for the protein content of each sample. An accurate titration with the uncoupler FCCP was performed, in order to utilize the FCCP concentration (20 nM) that maximally increases OCR.

Statistical analysis. Data were collected by investigators blinded to the experimental setup and were statistically analyzed by parametric Student's *t*-test. In all graphs, mean ± S.D. (standard deviation of the mean) are shown. *P*-values 0.01 were considered to be statistically significant. Statistical analysis was performed with Statgraphics Centurion XVI, version 16.1.12 (StatPoint Technologies, Inc. Warrenton, VA, USA)

Conflict of Interest

The authors declare no conflict of interest.

Acknowledgements. We thank Fabiola Pasqualato and Isabella Bortolato for technical assistance and for inexhaustible support. This work was made possible by grants from Progetti di Ateneo dell'Università di Padova and from the Associazione Italiana per la Ricerca sul Cancro (grant number 8722).

1. Hanahan D, Weinberg RA. The hallmarks of cancer. *Cell* 2000; **100**: 57–70.
2. Hanahan D, Weinberg RA. Hallmarks of cancer: the next generation. *Cell* 2011; **144**: 646–674.
3. Rasola A, Bernardi P. The mitochondrial permeability transition pore and its involvement in cell death and in disease pathogenesis. *Apoptosis* 2007; **12**: 815–833.
4. Youle RJ, Strasser A. The BCL-2 protein family: opposing activities that mediate cell death. *Nat Rev Mol Cell Biol* 2008; **9**: 47–59.
5. Yip KW, Reed JC. Bcl-2 family proteins and cancer. *Oncogene* 2008; **27**: 6398–6406.
6. Rasola A, Sciacovelli M, Pantic B, Bernardi P. Signal transduction to the permeability transition pore. *FEBS Lett* 2010; **584**: 1989–1996.
7. Masgras I, Rasola A, Bernardi P. Induction of the permeability transition pore in cells depleted of mitochondrial DNA. *Biochim Biophys Acta* 2012; **1817**: 1860–1866.
8. Rasola A, Sciacovelli M, Chiara F, Pantic B, Brusilow WS, Bernardi P. Activation of mitochondrial ERK protects cancer cells from death through inhibition of the permeability transition. *Proc Natl Acad Sci USA* 2010; **107**: 726–731.
9. Traba J, Del Arco A, Duchen MR, Szabadkai G, Satrustegui J. SCaMC-1 promotes cancer cell survival by desensitizing mitochondrial permeability transition via ATP/ADP-mediated matrix Ca(2 +) buffering. *Cell Death Differ* 2011; **19**: 650–660.
10. Levine AJ, Puzio-Kuter AM. The control of the metabolic switch in cancers by oncogenes and tumor suppressor genes. *Science* 2010; **330**: 1340–1344.
11. Hsu PP, Sabatini DM. Cancer cell metabolism: Warburg and beyond. *Cell* 2008; **134**: 703–707.
12. Warburg O. On the origin of cancer cells. *Science* 1956; **123**: 309–314.
13. Warburg O, Wind F, Negelein E. The metabolism of tumors in the body. *J Gen Physiol* 1927; **8**: 519–530.
14. Frezza C, Gottlieb E. Mitochondria in cancer: not just innocent bystanders. *Semin Cancer Biol* 2009; **19**: 4–11.
15. Murphy MP. How mitochondria produce reactive oxygen species. *Biochem J* 2009; **417**: 1–13.
16. Rasola A, Bernardi P. Mitochondrial permeability transition in Ca(2 +)-dependent apoptosis and necrosis. *Cell Calcium* 2011; **50**: 222–233.
17. Anastasiou D, Poulogiannis G, Asara JM, Boxer MB, Jiang JK, Shen M *et al.* Inhibition of pyruvate kinase M2 by reactive oxygen species contributes to cellular antioxidant responses. *Science* 2011; **334**: 1278–1283.
18. Cairns RA, Harris IS, Mak TW. Regulation of cancer cell metabolism. *Nat Rev Cancer* 2011; **11**: 85–95.
19. DeNicola GM, Karreth FA, Humpton TJ, Gopinathan A, Wei C, Frese K *et al.* Oncogene-induced Nrf2 transcription promotes ROS detoxification and tumorigenesis. *Nature* 2011; **475**: 106–109.
20. Ronconi L, Fregona D. The Midas touch in cancer chemotherapy: from platinum- to gold-dithiocarbamato complexes. *Dalton Trans* 2009; **48**: 10670–10680.
21. Ronconi L, Giovagnini L, Marzano C, Bettio F, Graziani R, Pilloni G *et al.* Gold dithiocarbamate derivatives as potential antineoplastic agents: design, spectroscopic properties, and *in vitro* antitumor activity. *Inorg Chem* 2005; **44**: 1867–1881.
22. Saggioro D, Rigobello MP, Paloschi L, Folda A, Moggach SA, Parsons S *et al.* Gold(III)-dithiocarbamato complexes induce cancer cell death triggered by thioredoxin redox system inhibition and activation of ERK pathway. *Chem Biol* 2007; **14**: 1128–1139.
23. Cattaruzza L, Fregona D, Mongiat M, Ronconi L, Fassina A, Colombatti A *et al.* Antitumor activity of gold(III)-dithiocarbamato derivatives on prostate cancer cells and xenografts. *Int J Cancer* 2011; **128**: 206–215.
24. Marzano C, Ronconi L, Chiara F, Giron MC, Faustinelli I, Cristofori P *et al.* Gold(III)-dithiocarbamato anticancer agents: activity, toxicology and histopathological studies in rodents. *Int J Cancer* 2011; **129**: 487–496.

25. Bello D, Webber MM, Kleinman HK, Wartinger DD, Rhim JS. Androgen responsive adult human prostatic epithelial cell lines immortalized by human papillomavirus 18. *Carcinogenesis* 1997; **18**: 1215–1223.
26. Webber MM, Bello D, Kleinman HK, Hoffman MP. Acinar differentiation by non-malignant immortalized human prostatic epithelial cells and its loss by malignant cells. *Carcinogenesis* 1997; **18**: 1225–1231.
27. Lemasters JJ, Theruvath TP, Zhong Z, Nieminen AL. Mitochondrial calcium and the permeability transition in cell death. *Biochim Biophys Acta* 2009; **1787**: 1395–1401.
28. Zorov DB, Juhaszova M, Sollott SJ, Mitochondrial ROS-induced ROS. Release: an update and review. *Biochim Biophys Acta* 2006; **1757**: 509–517.
29. Chiara F, Castellaro D, Marin O, Petronilli V, Brusilow WS, Juhaszova M *et al.* Hexokinase II detachment from mitochondria triggers apoptosis through the permeability transition pore independent of voltage-dependent anion channels. *PLoS ONE* 2008; **3**: e1852.
30. Lochhead PA, Kinstrie R, Sibbet G, Rawjee T, Morrice N, Cleghon V. A chaperone-dependent GSK3beta transitional intermediate mediates activation-loop autophosphorylation. *Mol Cell* 2006; **24**: 627–633.
31. Mathupala SP, Ko YH, Pedersen PL, Hexokinase II. Cancer's double-edged sword acting as both facilitator and gatekeeper of malignancy when bound to mitochondria. *Oncogene* 2006; **25**: 4777–4786.
32. Robey RB, Hay N. Mitochondrial hexokinases, novel mediators of the antiapoptotic effects of growth factors and Akt. *Oncogene* 2006; **25**: 4683–4696.
33. Beurel E, Jope RS. The paradoxical pro- and anti-apoptotic actions of GSK3 in the intrinsic and extrinsic apoptosis signaling pathways. *Prog Neurobiol* 2006; **79**: 173–189.
34. Jezek P, Hlavata L. Mitochondria in homeostasis of reactive oxygen species in cell, tissues, and organism. *Int J Biochem Cell Biol* 2005; **37**: 2478–2503.
35. Grek CL, Tew KD. Redox metabolism and malignancy. *Curr Opin Pharmacol* 2010; **10**: 362–368.
36. Trachootham D, Alexandre J, Huang P. Targeting cancer cells by ROS-mediated mechanisms: a radical therapeutic approach? *Nat Rev Drug Discov* 2009; **8**: 579–591.
37. Dang CV, Kim JW, Gao P, Yustein J. The interplay between MYC and HIF in cancer. *Nat Rev Cancer* 2008; **8**: 51–56.
38. Taylor CT. Mitochondria and cellular oxygen sensing in the HIF pathway. *Biochem J* 2008; **409**: 19–26.
39. Vousden KH, Ryan KM. p53 and metabolism. *Nat Rev Cancer* 2009; **9**: 691–700.
40. Chandar N, Billig B, McMaster J, Novak J. Inactivation of p53 gene in human and murine osteosarcoma cells. *Br J Cancer* 1992; **65**: 208–214.
41. Weinberg F, Hamanaka R, Wheaton WW, Weinberg S, Joseph J, Lopez M *et al.* Mitochondrial metabolism and ROS generation are essential for Kras-mediated tumorigenicity. *Proc Natl Acad Sci USA* 2010; **107**: 8788–8793.
42. Shaw AT, Winslow MM, Magendantz M, Ouyang C, Dowdle J, Subramanian A *et al.* Selective killing of K-ras mutant cancer cells by small molecule inducers of oxidative stress. *Proc Natl Acad Sci USA* 2011; **108**: 8773–8778.
43. Yagoda N, von Rechenberg M, Zaganjor E, Bauer AJ, Yang WS, Fridman DJ *et al.* RAS-RAF-MEK-dependent oxidative cell death involving voltage-dependent anion channels. *Nature* 2007; **447**: 864–868.
44. Sharma LK, Lu J, Bai Y. Mitochondrial respiratory complex I: structure, function and implication in human diseases. *Curr Med Chem* 2009; **16**: 1266–1277.
45. Efremov RG, Baradaran R, Sazanov LA. The architecture of respiratory complex I. *Nature* 2010; **465**: 441–445.
46. Baracca A, Chiaradonna F, Sgarbi G, Solaini G, Alberghina L, Lenaz G. Mitochondrial complex I decrease is responsible for bioenergetic dysfunction in K-ras transformed cells. *Biochim Biophys Acta* 2010; **1797**: 314–323.
47. Chen Y, McMillan-Ward E, Kong J, Israels SJ, Gibson SB. Mitochondrial electron-transport-chain inhibitors of complexes I and II induce autophagic cell death mediated by reactive oxygen species. *J Cell Sci* 2007; **120**: 4155–4166.
48. D'Autreaux B, Toledano MB. ROS as signalling molecules: mechanisms that generate specificity in ROS homeostasis. *Nat Rev Mol Cell Biol* 2007; **8**: 813–824.
49. Kaidanovich-Beilin O, Woodgett JR. GSK-3: functional insights from cell biology and animal models. *Front Mol Neurosci* 2011; **4**: 40.
50. Lin CL, Tseng HC, Chen RF, Chen WP, Su MJ, Fang KM *et al.* Intracellular zinc release-activated ERK-dependent GSK-3beta-p53 and Noxa-Mcl-1 signaling are both involved in cardiac ischemic-reperfusion injury. *Cell Death Differ* 2011; **18**: 1651–1663.
51. Vigneron F, Dos Santos P, Lemoine S, Bonnet M, Tariosse L, Couffinhal T *et al.* GSK-3beta at the crossroads in the signalling of heart preconditioning: implication of mTOR and Wnt pathways. *Cardiovasc Res* 2011; **90**: 49–56.
52. Wang SH, Shih YL, Kuo TC, Ko WC, Shih CM. Cadmium toxicity toward autophagy through ROS-activated GSK-3beta in mesangial cells. *Toxicol Sci* 2009; **108**: 124–131.
53. Lee KY, Koh SH, Noh MY, Park KW, Lee YJ, Kim SH. Glycogen synthase kinase-3beta activity plays very important roles in determining the fate of oxidative stress-inflicted neuronal cells. *Brain Res* 2007; **1129**: 89–99.
54. Walensky LD, Gavathiotis E. BAX unleashed: the biochemical transformation of an inactive cytosolic monomer into a toxic mitochondrial pore. *Trends Biochem Sci* 2011; **36**: 642–652.
55. Szabo I, Bock J, Grassme H, Soddemann M, Wilker B, Lang F *et al.* Mitochondrial potassium channel Kv1.3 mediates Bax-induced apoptosis in lymphocytes. *Proc Natl Acad Sci USA* 2008; **105**: 14861–14866.
56. Gramaglia D, Gentile A, Battaglia M, Ranzato L, Petronilli V, Fassetta M *et al.* Apoptosis to necrosis switching downstream of apoptosome formation requires inhibition of both glycolysis and oxidative phosphorylation in a BCL-X(L)- and PKB/AKT-independent fashion. *Cell Death Differ* 2004; **11**: 342–353.
57. Rasola A, Geuna M. A flow cytometry assay simultaneously detects independent apoptotic parameters. *Cytometry* 2001; **45**: 151–157.
58. Fontaine E, Eriksson O, Ichas F, Bernardi P. Regulation of the permeability transition pore in skeletal muscle mitochondria. Modulation by electron flow through the respiratory chain complex i. *J Biol Chem* 1998; **273**: 12662–12668.
59. Birch-Machin MA, Tumbull DM. Assaying mitochondrial respiratory complex activity in mitochondria isolated from human cells and tissues. *Methods Cell Biol* 2001; **65**: 97–117.

Supplementary Information accompanies the paper on Cell Death and Disease website (http://www.nature.com/cddis)